Capacitance of Dielectric Coated Cylinder of Finite Axial Length and Truncated Cone Isolated in Free Space

S. B. Chakrabarty, Sukhendu Das, and B. N. Das

***Abstract*—Capacitance of dielectric coated metallic cylinder and truncated cone are evaluated using the method of moments based on pulse function and point matching. The analysis is based on boundary condition for the potential on the conductor surface and normal component of displacement density at the dielectric-free space interface. The total free charge on the conductor surface is found from the inversion of a matrix partitioned into submatrices. Numerical data on capacitance and charge distribution are presented.**

***Index Terms*—Boundary value problem for dielectric coated cylinder isolated in free space, dielectric coated cylinder of finite length, dielectric coated truncated cone, evaluation of capacitance and charge distribution.**

I. Introduction

The capacitance of a cylinder of finite length and truncated cone in the presence of dielectric coating and isolated in free space can be found from the relation between the free charge on the conductor and its potential.

It is found from the analysis presented in references [1], [2] that in the presence of dielectric media there are free as well as bound charges on the conductor surface and bound charges on the dielectric surface. The charge distribution along the conductor surface is the sum of free charge and bound charge and the dielectric is electrically neutral. The potential on the conductor surface is related to charges on both these surfaces [1]–[3].

The method based on the replacement of surface charge by an axial charge distribution [4] can not be applied for finding the effect of dielectric coating on cylinder of finite length and truncated cone.

The capacitance of truncated cone and cylinder of finite length [5] has been found from the series combination of the capacitances of metal dielectric combination and dielectric to free space capacitance due to induced charge on the surface of the dielectric. The former capacitance has been found from the energy storage in the dielectric expressed in terms of displacement density due to free charge on the conductor surface. The later capacitance resulting from the unbalanced charge on the dielectric surface is found using moment method formulation based on pulse function as the basis function and point matching for testing.

In the method used in this paper, the surfaces of both the conductor and the dielectric are divided into curvilinear rectangular subsections using the method followed in [3]. The potential on the conductor surface is expressed in terms of distribution of total charge on the conductor surface and bound charge on the dielectric surface in the form of an integral equation. Another integral equation is obtained on satisfying the boundary condition for the normal component of displacement density at the air dielectric interface [1], [2]. These coupled integral equations are solved using pulse function for the unknown charge densities and point matching for testing [3]. The simultaneous equations so obtained lead to a matrix equation. The capacitance is found from the inversion of the matrix partitioned into submatrices [6, Sec. 24].

Manuscript received August 31, 2001; revised December 12, 2001. This work was supported by the Indian National Science Academy, New Delhi, India.

S. B. Chakrabarty is with MSAD/AFG/MISA, Space Applications Centre, Indian Space Research Organization, Ahmedabad 380 015, India.

S. Das is with the Department of Computer Science and Engineering, Indian Institute of Technology, Chennai 600036, India.

B. N. Das is with the Department of Electronics and Electrical Communication Engineering, Indian Institute of Technology, Kharagpur 721 302, India.

Publisher Item Identifier S 0018-9375(02)04552-0.

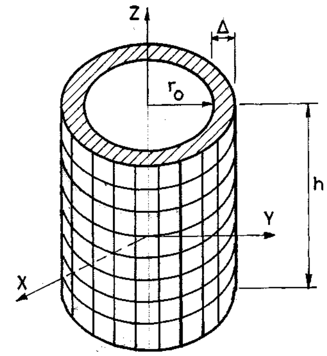

Fig. 1. A dielectric coated cylinder of finite length.

Numerical data on the capacitance as well as charge distribution are presented for cylinder, truncated cone in the presence of dielectric coating. The comparison of the data with those obtained by using other methods is presented.

II. General Analysis

A. Cylinder of Finite Length Coated With Uniform Dielectric

Fig. 1 shows a cylinder of axial length h, radius r_0 and dielectric of uniform width Δ, together with its coordinate system. The surfaces of the cylinder as well as the dielectric are divided into N cylindrical sections along the axis and M subsections along the circumference as shown in the same figure.

The potential at any arbitrary point due to charge distributions on the conductor (position vector r') and dielectric (position vector r'_*) surfaces is of the form [7], [8]

$$\Phi = \frac{1}{4\pi\epsilon_0}\left[\int_s \frac{\sigma(r', \phi', z')}{|r - r'|} + \int_{s^*} \frac{\sigma^*(r'_*, \phi'_*, z'_*)}{|r - r'_*|}\right] \quad (1)$$

where s and s^* represent integration over the conductor and dielectric surfaces, respectively.

The unknown charge distributions appearing in (1) are expressed in terms of known basis functions [8] as

$$\sigma(r') = \sum_{n=1}^{MN} \alpha_n f_n \quad (2)$$

$$\sigma^*(r'_*) = \sum_{n=MN+1}^{2MN} \alpha^*_n f_n \quad (3)$$

where f_n are the pulse functions given by

$$f_n = \begin{cases} 1, & \text{on } \Delta s_n \\ 0, & \text{on any other } \Delta s_m. \end{cases} \quad (4)$$

The radial component of electric field intensity at any point due to charge distribution on the conductor surface is given by

$$\vec{E} = -\vec{u}_r \frac{\partial \Phi}{\partial r} = \frac{1}{4\pi\epsilon_0}\int_s \frac{(r - r')\sigma(r', \phi', z')}{|r - r'|^3}. \quad (5)$$

Substituting (2) and (3) in (1) and matching the boundary conditions for the potential at the center point of each curvilinear subsection and following the procedure of [3], the equation reduces to the form

$$V = \sum_{n=1}^{MN} \alpha_n l_{11mn} + \sum_{n=MN+1}^{2MN} \alpha^*_n l_{12mn}, \quad m = 1, \ldots, MN. \quad (6)$$

Using (2), (3), and (5), and continuity of the radial component of displacement density leads to the following equation [1]–[3]

$$0 = \sum_{n=1}^{MN} \alpha_n l^*_{21mn} - \frac{1}{\epsilon_0(\epsilon_r - 1)} \sum_{n=MN+1}^{2MN} \alpha^*_n l^*_{22mn}, \quad m = MN+1, \ldots, 2MN \tag{7}$$

where

$$l^*_{22mn} = \begin{cases} 1, & m = n \\ 0, & m \neq n. \end{cases}$$

MN is the total number of curvilinear rectangular subareas into which each surfaces of conductor and dielectric are divided.

The coefficients appearing in (6) and (7) are found to be of the form as shown in (8)–(10) at the bottom of the page, where

$$\cos\psi = \frac{(r_0+\Delta) - r_0 \cos\left((m-n)\,\frac{2\pi}{M}\right)}{\sqrt{r_0^2 + (r_0+\Delta)^2 - 2r_0(r_0+\Delta)\cos\left((m-n)\,\frac{2\pi}{M}\right)}} \tag{11}$$

and Δ is the width of the dielectric coating on the cylinder of Fig. 1. Equations (8)–(10) are valid for $m \neq n$.

The set of simultaneous equations resulting from (6) and (7) lead to a matrix equation of the from

$$\begin{bmatrix} [l_{11mn}] & [l_{12mn}] \\ [l^*_{21mn}] & \left[-\frac{1}{\epsilon_0(\epsilon_r-1)}\, l^*_{22mn}\right] \end{bmatrix} \begin{bmatrix} [\alpha_n] \\ [\alpha^*_n] \end{bmatrix} = \begin{bmatrix} [V] \\ [0] \end{bmatrix} \tag{12}$$

where $[l_{11mn}]$, $[l_{12mn}]$, $[l^*_{21mn}$, $[l^*_{22mn}]$ are the submatrices each of order $MN \times MN$ and $[l^*_{22mn}]$ is the unit matrix, $[V]$ and [0] are the column submatrices each of order $MN \times 1$.

Following the procedure suggested in [7, Appendix E], the diagonal elements of submatrices $[l_{11mn}]$ and $[l_{12mn}]$ are obtained from the formula

$$l_{11nn} = \frac{1}{2\pi\epsilon_0}\left[\frac{2\pi r_0}{M}\ln\left\{\frac{hM}{2\pi r_0 N} + \sqrt{1+\left(\frac{hM}{2\pi r_0 N}\right)^2}\right\} + \frac{h}{N}\ln\left\{\frac{2\pi r_0 N}{Mh} + \sqrt{1+\left(\frac{2\pi r_0 N}{Mh}\right)^2}\right\}\right] \tag{13}$$

$$l_{12nn} = \frac{1}{4\pi\epsilon_0}\left\{Z\ln\left[\frac{X+Y}{-X+Y}\right] + X\ln\left[\frac{Z+Y}{-Z+Y}\right] - 4D\tan^{-1}\frac{XZ}{2DY}\right\} \tag{14}$$

where

$$X = \frac{h}{N}, \quad Z = \frac{2\pi r}{M}$$
$$Y = \sqrt{X^2+Z^2+4D^2}, \quad D = r - r_0.$$

Substituting $r = r_0 + \Delta$ in (14), the diagonal elements l_{12nn} are obtained.

The diagonal elements of $[l^*_{21mn}]$ are obtained on differentiating (14) with respect to r and substituting $r = r_0 + \Delta$ and hence

$$l^*_{21mn} = -\frac{\partial}{\partial r}(l_{12mn})\bigg|_{r=r_0+\Delta}.$$

With the substitution $a = h/N$, $b = 2\pi r_0/M$, the expression for the diagonal elements assumes the form [7]

$$l^*_{21mn} = \frac{1}{4\pi\epsilon_0} \cdot \left[\frac{4ab(r_0+\Delta)(a^2+b^2+2\Delta^2)}{\sqrt{a^2+b^2+2\Delta^2}(a^2+\Delta^2)(b^2+\Delta^2)} + p_1 + p_2\right] \tag{15}$$

where

$$p_1 = \frac{-4ab\Delta(a^2+b^2+\Delta^2+\Delta(r_0+\Delta))}{[\Delta^2(a^2+b^2+\Delta^2)+a^2b^2]\sqrt{a^2+b^2+\Delta^2}}$$

$$p_2 = 4\tan^{-1}\frac{ab}{\Delta\sqrt{a^2+b^2+\Delta^2}}.$$

Using the method suggested in the literature for inversion of a matrix by partitioning it into submatrices [6], the solution of (12) is obtained as

$$\begin{bmatrix} [\alpha_n] \\ [\alpha^*_n] \end{bmatrix} = \begin{bmatrix} [\xi_{11mn}] & [\xi_{12mn}] \\ [\xi_{21mn}] & [\xi_{22mn}] \end{bmatrix} \begin{bmatrix} [V] \\ [0] \end{bmatrix} \tag{16}$$

where ξ_{mn} are the elements of inverse of the square matrix of equation (12). The inverse matrix is again partitioned into sub-matrices $[\xi_{11mn}]$, $[\xi_{12mn}]$, $[\xi_{21mn}]$, $[\xi_{22mn}]$.

The total free charge on the surface of the conductor is

$$Q = \sum_{n=1}^{MN}\sum_{n=1}^{MN}\left[\alpha_n\,\frac{2\pi r_0 h}{MN} + \alpha^*_n\,\frac{2\pi(r_0+\Delta)h}{MN}\right]. \tag{17}$$

The capacitance per unit length of the structure shown in Fig. 1 is

$$C = \frac{1}{h}\,\frac{Q}{V}. \tag{18}$$

III. Truncated Cone With Uniform Dielectric Coating

A truncated cone with radii r_1 and r_2 at the uppermost and lowermost cross-sections and axial length h together with the coordinate system is shown in Fig. 2. The conductor of uniform thickness is approximated by a combination of N cylindrical sections along the axis [4].

The radius of the nth cylindrical section on the conducting surface is given by

$$r_n = r_2 + \frac{r_1 - r_2}{h}\,z(n) \tag{19}$$

where $z(n) = (n-1)(h/N) + (h/2N)$.

$$l_{11mn} = \frac{1}{4\pi\epsilon_0}\,\frac{(2\pi r_0 h)/MN}{\sqrt{4r_0^2\sin^2\left((m-n)\,\frac{\pi}{M}\right) + \left((m-n)\,\frac{h}{N}\right)^2}} \tag{8}$$

$$l_{12mn} = \frac{1}{4\pi\epsilon_0}\,\frac{(2\pi(r_0+\Delta)h)/MN}{\sqrt{r_0^2 + (r_0+\Delta)^2 - 2r_0(r_0+\Delta)\cos\left((m-n)\,\frac{2\pi}{M}\right) + \left((m-n)\,\frac{h}{N}\right)^2}} \tag{9}$$

$$l^*_{21mn} = \frac{1}{4\pi\epsilon_0}\,\frac{(2\pi(r_0+\Delta)h/MN)\cos\psi}{r_0^2 + (r_0+\Delta)^2 - 2r_0(r_0+\Delta)\cos\left((m-n)\,\frac{2\pi}{M}\right) + \left((m-n)\,\frac{h}{N}\right)^2} \tag{10}$$

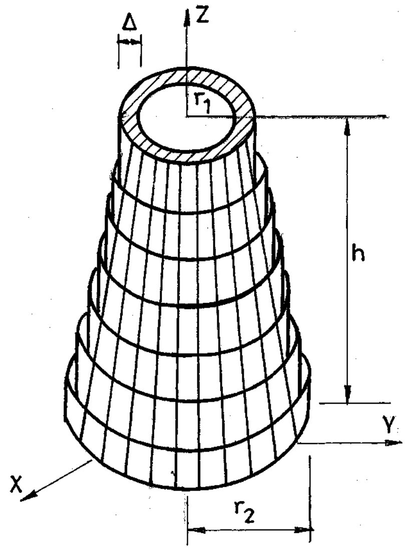

Fig. 2. A dielectric coated truncated cone.

The radius of the nth cylindrical section on the surface of the dielectric is

$$r_n^\Delta = r_n + \Delta. \tag{20}$$

Each cylindrical segment on both the surfaces is divided into M subsections along the circumference, uniformly along the axis. The circumferential dimension of the curvilinear rectangles depends upon the radii and is different along the axial direction for conductor and dielectric surfaces, uniformly along the axis. The circumferential dimension of the curvilinear rectangles depends upon the radii and is different along the axial direction for conductor and dielectric surfaces.

Following the procedure of Section II-A, the matrix equation for this problem is obtained as shown

$$\begin{bmatrix} [L_{11mn}] & [L_{12mn}] \\ [L^*_{21mn}] & \left[-\frac{1}{\epsilon_0(\epsilon_r - 1)} L^*_{22mn}\right] \end{bmatrix} \begin{bmatrix} [\beta_n] \\ [\beta^*_n] \end{bmatrix} = \begin{bmatrix} [V_t] \\ [0] \end{bmatrix}. \tag{21}$$

The elements of the submatrices appearing in the left-hand side of the above equation are shown in (22)–(24) at the bottom of the page, where

$$\cos\psi = \frac{(r_n + \Delta) - r_n \cos\left((m-n)\frac{2\pi}{M}\right)}{\sqrt{r_n^2 + (r_n+\Delta)^2 - 2r_n(r_n+\Delta)\cos\left((m-n)\frac{2\pi}{M}\right)}}. \tag{25}$$

Δ is the width of the dielectric coating on the cylinder of Fig. 1. Equations (22)–(25) are valid for $m \neq n$.

$[L^*_{22mn}]$ is the unit matrix, $[V_t]$ and [0] are the column matrices.

The diagonal elements are as follows:

$$L_{11nn} = \frac{1}{2\pi\epsilon_0}\left[\frac{2\pi r_n}{M}\ln\left\{\frac{hM}{2\pi r_n N} + \sqrt{1 + \left(\frac{hM}{2\pi r_n N}\right)^2}\right\} + \frac{h}{N}\ln\left\{\frac{2\pi r_n N}{Mh} + \sqrt{1+\left(\frac{2\pi r_n N}{Mh}\right)^2}\right\}\right] \tag{26}$$

$$L_{12nn} = \frac{1}{4\pi\epsilon_0}\left\{Z\ln\left[\frac{X+Y}{-X+Y}\right] + X\ln\left[\frac{Z+Y}{-Z+Y}\right] - 4D\tan^{-1}\frac{XZ}{2DY}\right\} \tag{27}$$

where

$$X = \frac{h}{N}, \quad Z = \frac{2\pi r^n}{M}$$
$$Y = \sqrt{X^2 + Z^2 + 4D^2}, \quad D = r^n - r_n.$$

Substituting $r^n = r_n + \Delta$ in (27), the diagonal elements L_{12nn} are obtained.

The diagonal elements of $[L^*_{21mn}]$ are obtained on differentiating (27) with respect to r^n and substituting $r^n = r_n + \Delta$ and hence

$$L^*_{21mn} = -\frac{\partial}{\partial r^n}(l_{12mn})\Big|_{r^n = r_n + \Delta}.$$

Following the similar method as applied in Section II-A, the unknown charge densities β_n and β^*_n are evaluated from the inversion of the matrix equation (21) by partitioning it into submatrices and is obtained as under

$$\begin{bmatrix} [\beta_n] \\ [\beta^*_n] \end{bmatrix} = \begin{bmatrix} [\xi^{ll}_{mn}] & [\xi^{lr}_{mn}] \\ [\xi^{rl}_{mn}] & [\xi^{rr}_{mn}] \end{bmatrix} \begin{bmatrix} [V_t] \\ [0] \end{bmatrix} \tag{28}$$

where ξ_{mn} are the elements of inverse of the square matrix of equation (28).

The total charge on the conductor surface is given by

$$Q = \sum_{n=1}^{MN}\sum_{n=1}^{MN}\left[\beta_n \frac{2\pi r_n h}{MN} + \beta^*_n \frac{2\pi(r_n+\Delta)h}{MN}\right]. \tag{29}$$

The capacitance per unit length of the structure shown in Fig. 2 is

$$C' = \frac{1}{h}\frac{Q}{V_t}. \tag{30}$$

IV. Numerical Results

Using equations (8)–(18), the capacitance per unit length of the dielectric coated cylinder of Fig. 1 is evaluated as a function of h/r_0 with Δ/h as a parameter for $\epsilon_r = 3.0$. The convergence of the numerical data on the capacitance per unit length is checked for each parameter. A representative convergence data for the dielectric coated cylinder is shown in Table I.

$$L_{11mn} = \frac{1}{4\pi\epsilon_0}\frac{(2\pi r_n h)/MN}{\sqrt{4r_n^2\sin^2\left((m-n)\frac{\pi}{M}\right) + \left((m-n)\frac{h}{N}\right)^2}} \tag{22}$$

$$L_{12mn} = \frac{1}{4\pi\epsilon_0}\frac{(2\pi(r_n+\Delta)h)/MN}{\sqrt{r_n^2 + (r_n+\Delta)^2 - 2r_n(r_n+\Delta)\cos\left((m-n)\frac{2\pi}{M}\right) + \left((m-n)\frac{h}{N}\right)^2}} \tag{23}$$

$$L^*_{21mn} = \frac{1}{4\pi\epsilon_0}\frac{(2\pi(r_n+\Delta)h/MN)\cos\psi}{r_n^2 + (r_n+\Delta)^2 - 2r_n(r_n+\Delta)\cos\left((m-n)\frac{2\pi}{M}\right) + \left((m-n)\frac{h}{N}\right)^2} \tag{24}$$

TABLE I
CONVERGENCE OF THE CAPACITANCE/LENGTH OF DIELECTRIC COATED CYLINDER FOR $h/r_0 = 40$

M	N	Capacitance/ length (pf/m)
3	18	21.67
4	24	21.69
5	30	22.15
6	36	22.68
7	42	22.79

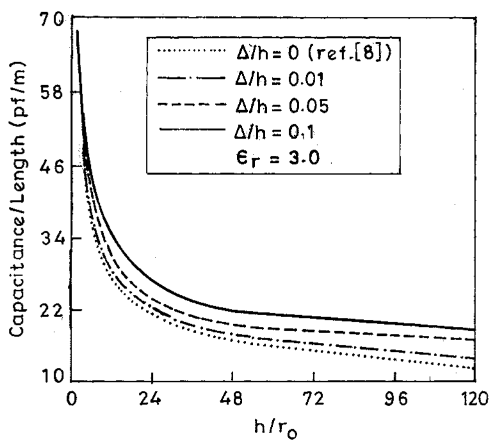

Fig. 3. The capacitance per unit length of a dielectric coated metallic cylinder as a function of h/r_0 with Δ/h as a parameter and $\epsilon_r = 3.0$.

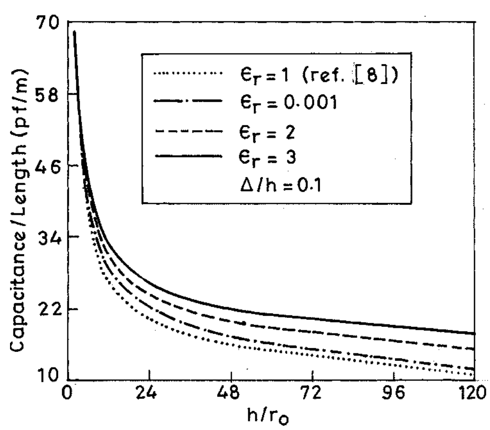

Fig. 4. The capacitance per unit length of a dielectric coated metallic cylinder as a function of h/r_0 with $\epsilon_r = 3.0$ and $\Delta/h = 0.1$.

The variation of the numerical results on capacitance per unit length of the cylinder of Fig. 1 with h/r_0 and Δ/h as a parameter are presented in Fig. 3.

Fig. 4 presents a variation of numerical results on capacitance per unit length with h/r_0 for $\Delta/h = 0.1$ and ϵ_r as a parameter. For the sake of comparison, the numerical data evaluated by the present method for $\Delta = 0$ and those available from [8] are also included in Figs. 3 and 4.

The axial charge distribution on the conductor and dielectric surfaces for the cylinder of Fig. 1 is shown in Fig. 5 for $\Delta/h = 0.1, h/r_0 = 2.0$, $\epsilon_r = 3.0$ and $V = 1$ V.

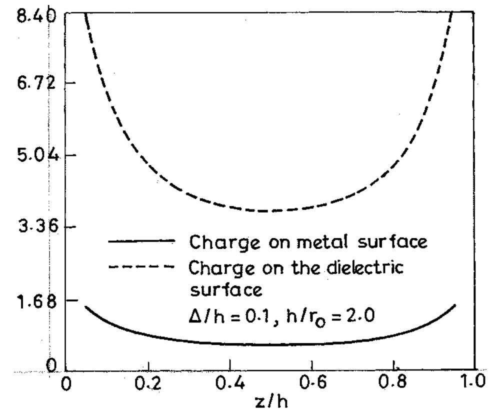

Fig. 5. The charge per unit length on the metal as well as on the dielectric surface of the dielectric coated metallic cylinder as a function of axial distance normalized with respect to h for $\Delta/h = 0.1, h/r_0 = 2.0$ and $V = 1$ V.

TABLE II
CONVERGENCE OF THE CAPACITANCE/LENGTH OF DIELECTRIC COATED TRUNCATED CONE FOR $h/r_2 = 40, \Delta/h = 0.1, r_2/r_1 = 0.85, \epsilon_r = 3.0$

M	N	Capacitance/ length (pf/m)
2	13	21.72
31	20	22.76
4	26	22.84
5	33	22.91
6	39	22.96
7	46	23.06

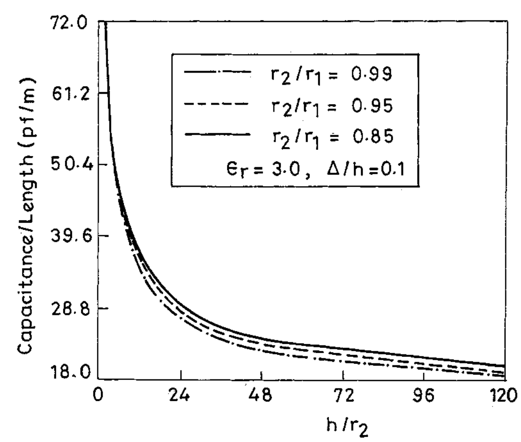

Fig. 6. The capacitance per unit length of a dielectric coated truncated cone as function of h/r_2 with $r_2/r_1 = 0.99, 0.95, 0.85$ and $\epsilon_r = 3.0, \Delta/h = 0.1$.

The convergence of the numerical data on the capacitance per unit length of a truncated cone was achieved for each parameter set. The convergence data for $h/r_2 = 40, \Delta/h = 0.1, r_2/r_1 = 0.85, \epsilon_r = 3.0$. These data are shown in Table II.

Using equations (19)–(30), the capacitance per unit length of a truncated cone was evaluated as a function of h/r_2 with r_2/r_1 as a parameter, $\epsilon_r = 3.0, \Delta/h = 0.1$. These data are shown in Fig. 6. The results on the capacitance for $r_2/r_1 = 0.99$, $\Delta/h = 0.01$ and $\epsilon_r = 3.0$ are shown in Fig. 7. The axial charge distribution on the conductor

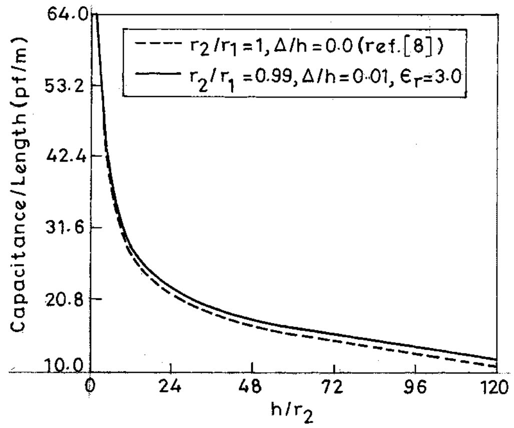

Fig. 7. The capacitance per unit length of a dielectric coated truncated cone as function of h/r_2 with $r_2/r_1 = 1$, 0.99 and $\epsilon_r = 3.0$, $\Delta/h = 0.01$.

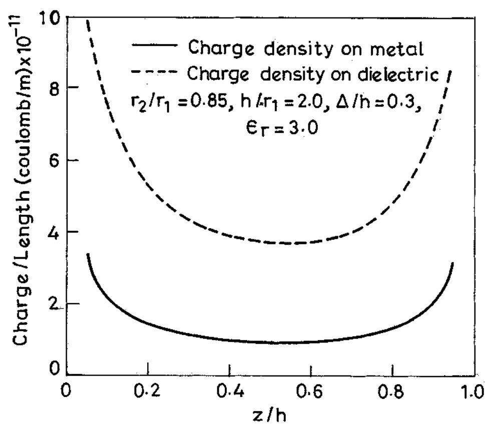

Fig. 8. The charge per unit length on the metal as well as on the dielectric surface of the dielectric coated truncated cone as a function of axial distance normalized with respect to h for $r_2/r_1 = 0.85$ and $\epsilon_r = 3.0$, $\Delta/h = 0.1$, $h/r_1 = 2.0$ and $V = 1$ V.

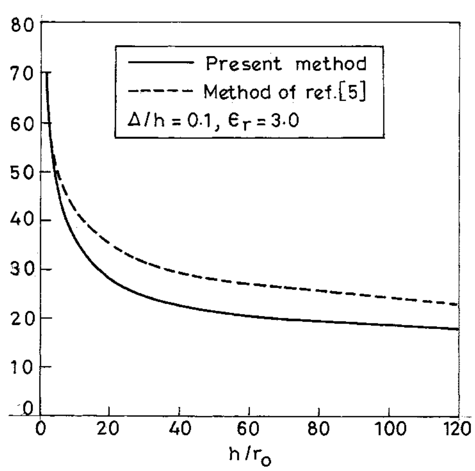

Fig. 9. Comparison of the capacitance data presented in ref. [5] for a dielectric coated cylinder with that of the present method for $\Delta/h = 0.1$ and $\epsilon_r = 3.0$.

and dielectric surfaces for the structure of Fig. 2 for $r_2/r_1 = 0.85$, $h/r_1 = 2.0$, $\Delta/h = 0.1$ and $\epsilon_r = 3.0$ are presented in Fig. 8. A comparison of the data of [5] is presented in Figs. 9 and 10.

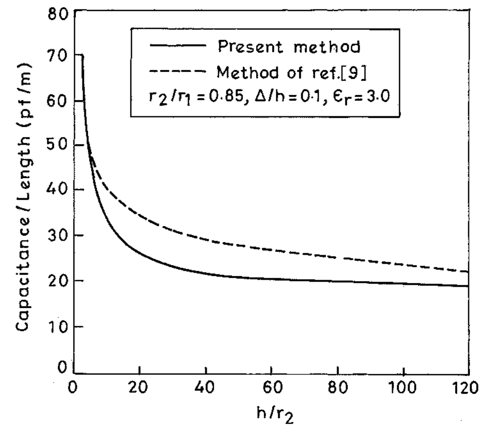

Fig. 10. Comparison of the capacitance data presented in ref. [5] for a dielectric coated cylinder with that of the present method for $r_2/r_1 = 0.85$, $\Delta/h = 0.1$ and $\epsilon_r = 3.0$.

V. Discussion

Agreement of the results with those of Harrington [8] for $\Delta = 0$ in the cases of cylinder and truncated cone for $r_2/r_1 = 1$ justifies the validity of the analysis. For both cylinders and truncated cone, the capacitance per unit length decreases with increase in h/r_0. For a particular value of h/r_0, the capacitance per unit length of the cylinder increases with increase in width of the dielectric above the conductor surface. In case of a truncated cone, the capacitance per unit length tends to increase with decrease in r_2/r_1 ratio for higher values of h/r_2. This can be attributed to the increase in surface area over which the charge is distributed.

Figs. 9 and 10 shows fairly good agreement of the data on capacitance computed by the present method and [5] for the identical geometrical parameters.

Acknowledgment

The authors would like to thank the anonymous reviewers for their useful comments and suggestions.

References

[1] J. C. Clements, C. R. Paul, and A. T. Adams, "Computation of capacitance matrix for systems of dielectric coated cylindrical conductors," *IEEE Trans. Electromagn. Compat.*, vol. EMC-17, pp. 238–248, Nov. 1975.
[2] J. S. Savage and W. S. Smith, "Capacitance calculation for cable harness using the method of moments," *IEEE Trans. Electromagn. Compat.*, vol. EMC-37, pp. 131–137, Feb. 1995.
[3] B. N. Das and S. B. Chakrabarty, "Capacitance and charge distribution of two cylindrical conductors of finite length," *Proc. Inst. Elect. Eng. Sci., Meas. Technol.*, vol. 144, no. 6, pp. 280–286, 1997.
[4] C. Chakrabarty, D. R. Poddar, A. Chakrabarty, and B. N. Das, "Electrostatic charge distribution and capacitance of isolated cylinders and truncated cones in free space," *IEEE Trans. Electromagn. Compat.*, vol. EMC-35, pp. 98–102, Feb. 1993.
[5] B. N. Das and S. B. Chakrabarty, "Rigorous analysis of the effect of dielectric coating on metallic bodies isolated in free space," *Proc. Indian Nat. Sci. Acad. A*, vol. 64, A, no. 2, pp. 137–148, 1998.
[6] E. A. Guillemin, *Mathematics of Circuit Analysis*. Cambridge, MA: Publishing, M.I.T Press, 1962, ch. 6.
[7] A. T. Adams, *Electromagnetics for Engineers*. New York: Ronald, 1972.
[8] R. F. Harrington, *Field Computation by Moment Methods*. New York: Macmillan, 1968.